

*Engineering*

*Electrical Engineering fields*

---

Okayama University

Year 1997

---

The unified power quality conditioner:  
the integration of series and shunt-active  
filters

Hideaki Fujita  
Okayama University

Hirofumi Akagi  
Okayama University

This paper is posted at eScholarship@OUDIR : Okayama University Digital Information Repository.

[http://escholarship.lib.okayama-u.ac.jp/electrical\\_engineering/15](http://escholarship.lib.okayama-u.ac.jp/electrical_engineering/15)

# The Unified Power Quality Conditioner: The Integration of Series- and Shunt-Active Filters

Hideaki Fujita, *Member, IEEE*, and Hirofumi Akagi, *Fellow, IEEE*

**Abstract**—This paper deals with unified power quality conditioners (UPQC's), which aim at the integration of series-active and shunt-active filters. The main purpose of a UPQC is to compensate for voltage flicker/imbalance, reactive power, negative-sequence current, and harmonics. In other words, the UPQC has the capability of improving power quality at the point of installation on power distribution systems or industrial power systems.

This paper discusses the control strategy of the UPQC, with a focus on the flow of instantaneous active and reactive powers inside the UPQC. Experimental results obtained from a laboratory model of 20 kVA, along with a theoretical analysis, are shown to verify the viability and effectiveness of the UPQC.

**Index Terms**—Active filters, harmonics, power conditioners, power quality, voltage flicker, voltage imbalance.

## I. INTRODUCTION

A SPECIALLY designed 12-pulse thyristor rectifier of 5–8 MVA is required to generate a strong magnetic field with high stability as a low-voltage high-current dc power supply for super-conductive material tests, proton synchrotron accelerators, and so on. The thyristor rectifier has to be equipped with a filter consisting of reactors and capacitors on its dc terminals to prevent current ripples from flowing into the electromagnet. The filter can easily eliminate high-frequency current ripples accompanying ac/dc power conversion. It is, however, difficult to reduce low-frequency current ripples caused by a supply voltage flicker with a frequency range from 1 to 20 Hz. It is pointed out that such a voltage flicker appearing at the point of common coupling (PCC) results from large capacity arc furnaces and/or cycloconverters installed on the same or upstream power system.

This paper deals with unified power quality conditioners (UPQC's) [1]–[3], which aim at the integration of series-active [4]–[7] and shunt-active filters. The main purpose of a UPQC is to compensate for supply voltage flicker/imbalance, reactive power, negative-sequence current, and harmonics. In other words, the UPQC has the capability of improving power quality at the point of installation on power distribution systems or industrial power systems. The UPQC, therefore, is expected to be one of the most powerful solutions to large capacity loads sensitive to supply voltage flicker/imbalance.

This paper presents two types of UPQC's. One is a general UPQC for power distribution systems and industrial power

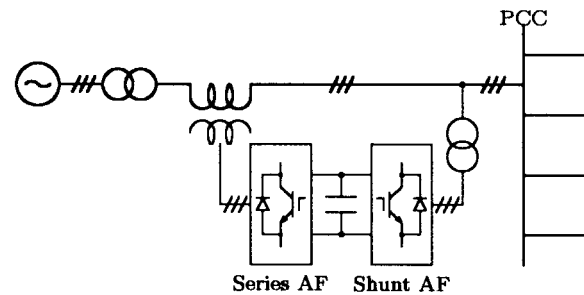


Fig. 1. General UPQC.

systems. The other is a specific UPQC for a supply voltage-flicker/imbalance-sensitive load, which is installed by electric power consumers on their own premises. In this paper, much attention is paid to the specific UPQC consisting of a series-active and shunt-active filter. The series-active filter eliminates supply voltage flicker/imbalance from the load terminal voltage, and forces an existing shunt-passive filter to absorb all the current harmonics produced by a nonlinear load. Elimination of supply voltage flicker, however, is accompanied by low-frequency fluctuation of active power flowing into or out of the series-active filter. The shunt-active filter performs dc-link voltage regulation, thus leading to a significant reduction of capacity of the dc capacitor. This paper reveals the flow of instantaneous active and reactive powers inside the UPQC and shows experimental results obtained from a laboratory model of 20 kVA.

## II. GENERAL UPQC

Fig. 1 shows a basic system configuration of a general UPQC consisting of the combination of a series-active and shunt-active filter [1]. The general UPQC will be installed at substations by electric power utilities in the near future. The main purpose of the series-active filter is harmonic isolation between a subtransmission system and a distribution system. In addition, the series-active filter has the capability of voltage-flicker/imbalance compensation as well as voltage regulation and harmonic compensation at the utility-consumer point of common coupling (PCC). The main purpose of the shunt-active filter is to absorb current harmonics, compensate for reactive power and negative-sequence current, and regulate the dc-link voltage between both active filters.

In this paper, the integration of the series-active and shunt-active filters is called the UPQC, associated with the unified power flow controller which has been proposed by Gyugyi [8]. However, the UPQC for distribution systems is quite different

Manuscript received May 6, 1996; revised July 29, 1997. Recommended by Associate Editor, L. Xu.

The authors are with the Department of Electrical Engineering, Okayama University, Okayama 700, Japan.

Publisher Item Identifier S 0885-8993(98)01946-2.

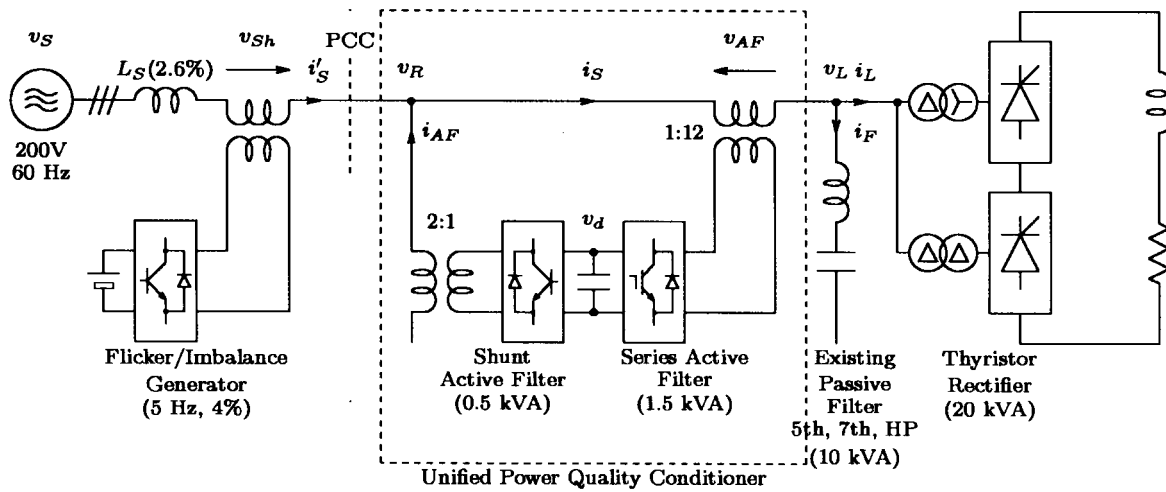


Fig. 2. Specific UPQC used in experiment.

in purpose, operation, and control strategy from the unified power flow controller for transmission systems.

### III. EXPERIMENTAL SYSTEM

Fig. 2 shows an experimental system configuration of a specific UPQC. The aim of the specific UPQC is not only to compensate for the current harmonics produced by a 12-pulse thyristor rectifier of 20 kVA, but also to eliminate the voltage flicker/imbalance contained in the receiving terminal voltage  $v_R$  from the load terminal voltage  $v_L$ . The receiving terminal in Fig. 2 is often corresponding to the utility-consumer point of common coupling in high-power applications. The UPQC consists of a 1.5-kVA series-active filter and a 0.5-kVA shunt-active filter. The dc links of both active filters are connected to a common dc capacitor of 2000  $\mu\text{F}$ . The 12-pulse thyristor bridge rectifier is considered a voltage-flicker/imbalance-sensitive load identical to a dc power supply for super-conductive material tests.

The power circuit of the 1.5-kVA series-active filter consists of three single-phase H-bridge voltage-fed pulse-width-modulation (PWM) inverters using four insulated gate bipolar transistors (IGBT's) in each phase. The operation of the series-active filter greatly forces all the current harmonics produced by the thyristor rectifier into an existing shunt-passive filter of 10 kVA. It also has the capability of damping series/parallel resonance between the supply impedance and the shunt-passive filter.

The 0.5-kVA shunt-active filter consisting of a three-phase voltage-fed PWM inverter is connected in parallel to the supply by a step-up transformer. The only objective of the shunt-active filter is to regulate the dc-link voltage between both active filters. Thus, the dc link is kept as a constant voltage even when a large amount of active power is flowing into or out of the series-active filter during the flicker compensation. Although the shunt-active filter has the capability of reactive power compensation, the shunt-active filter in Fig. 2 provides no reactive power compensation in order to achieve the minimum required rating of the shunt-active filter.

The circuit constants of the 10-kVA shunt-passive filter are shown in Table I. The filter consists of 5th- and 7th-tuned filters and a high-pass filter for the purpose of harmonic compensation of the 20-kVA 12-pulse thyristor rectifier. The 12-pulse thyristor rectifier practically produces a nonnegligible amount of 5th- and 7th-order harmonic currents, not only due to an error or imbalance in the firing angle between the two six-pulse thyristor rectifiers, but also due to a mismatch in the leakage inductance and/or the turn ratio between the two three-phase transformers interfacing the upper and lower rectifiers to the utility. The 5th- and 7th-order harmonic currents amplified as a result of resonance between the supply inductance and the passive filter would flow upstream of the PCC if neither 5th- nor 7th-tuned filter were installed. To damp the harmonic amplification caused by the resonance, 5th- and/or 7th-tuned filters are commonly installed in large-capacity 12-pulse thyristor rectifiers.

There is a notable difference in the installation point of the shunt-active filter between Figs. 1 and 2. The reason is clarified as follows: In Fig. 1, the shunt-active filter compensates for all the current harmonics produced by nonlinear loads downstream of the PCC. Therefore, it should be connected downstream of the series-active filter acting as a high resistor for harmonic frequencies. In Fig. 2, the shunt-active filter draws or injects the active power fluctuating at a low frequency from or into the supply, while the existing shunt-passive filter absorbs the current harmonics. To avoid interference between the shunt-active and passive filters, the shunt-active filter should be connected upstream of the series-active filter.

A three-phase voltage-fed PWM inverter connected in series with the supply is used as a voltage-flicker/imbalance generator in this experiment.

### IV. COMPENSATION STRATEGY

Fig. 3 shows a single-phase equivalent circuit for Fig. 2. For the sake of simplicity, the shunt-active filter is removed from Fig. 3 because it has no effect on harmonic and flicker compensation. Three kinds of control methods are discussed as follows:

TABLE I  
CIRCUIT CONSTANTS OF EXISTING SHUNT-PASSIVE FILTER

	$L$ [mH]	$C$ [ $\mu$ F]	$Q$	Capacity
5th	1.1	260	30	4 kVA
7th	1.1	130	30	2 kVA
HPF	0.19	260	—	4 kVA

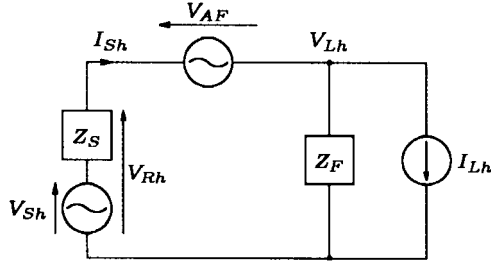


Fig. 3. Equivalent circuit for harmonics.

1) current-detecting method

$$V_{AF}^* = K \cdot I_{Sh} \quad (1)$$

2) voltage-detecting method

$$V_{AF}^* = V_{Rh} \quad (2)$$

3) combined method

$$V_{AF}^* = K \cdot I_{Sh} + V_{Rh} \quad (3)$$

where  $K$  is a proportional gain with a real number.

#### A. Current-Detecting Method

Fig. 4 shows an equivalent circuit, where the current-detecting method is applied. Equation (1) means that the series-active filter acts as a resistor of  $K$  [ $\Omega$ ] for harmonics. The load terminal voltage harmonics  $V_{Lh}$  and the supply current harmonics  $I_{Sh}$  are given as follows:

$$V_{Lh} = \frac{Z_F}{Z_S + Z_F + K} V_{Sh} - \frac{Z_S + K}{Z_S + Z_F + K} Z_F I_{Lh} \quad (4)$$

$$I_{Sh} = \frac{1}{Z_S + Z_F + K} V_{Sh} + \frac{Z_F}{Z_S + Z_F + K} I_{Lh}. \quad (5)$$

If the feedback gain  $K$  is set as  $K \gg Z_S + Z_F$ , neither voltage harmonics nor voltage flicker appears at the load terminal, irrespective of voltage harmonics and flicker existing at the receiving terminal. Then a small amount of harmonic voltage  $Z_F I_{Lh}$  is included in  $V_{Lh}$ . However, no voltage flicker is contained in  $V_{Lh}$  because a thyristor rectifier essentially produces no current flicker if no voltage flicker exists. As a result, both the load terminal voltage and the supply current become purely sinusoidal. It is, however, difficult to set  $K$  much larger than  $Z_S + Z_F$  for voltage flicker because  $Z_F$  exhibits high capacitive impedance at the fundamental frequency. Thus, the current-detecting method in (1) is not suitable for voltage-flicker compensation.

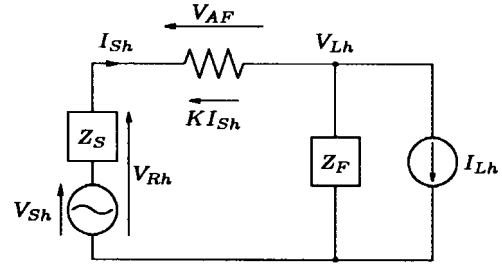


Fig. 4. Equivalent circuit for current-detecting method.

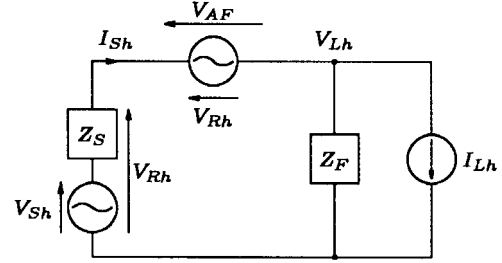


Fig. 5. Equivalent circuit for voltage-detecting method.

#### B. Voltage-Detecting Method

Fig. 5 shows an equivalent circuit based on the voltage-detecting method in (2). Because the output voltage of the series-active filter  $V_{AF}$  cancels the receiving terminal voltage harmonics  $V_{Rh}$ , neither supply voltage harmonics nor supply voltage flicker appears at the load terminal, that is,

$$V_{Lh} = 0. \quad (6)$$

However, the existing shunt-passive filter loses the capability of trapping current harmonics, so that all the current harmonics produced by the load escape to the supply, that is,

$$I_{Sh} = I_{Lh}. \quad (7)$$

Thus, the voltage-detecting method in (2) is not suitable for harmonic compensation of the load.

#### C. Combined Method

Fig. 6 shows an equivalent circuit combining the circuits in Figs. 4 and 5. It is clear from (3) that the series-active filter looks like a series connection of a voltage source  $V_{Rh}$  and a resistor  $K$  [ $\Omega$ ]. The receiving terminal voltage harmonics  $V_{Rh}$  and supply current harmonics  $I_{Sh}$  are given by the following:

$$V_{Lh} = -\frac{K Z_F}{Z_F + K} I_{Lh} \quad (8)$$

$$I_{Sh} = \frac{Z_F}{Z_F + K} I_{Lh}. \quad (9)$$

If  $K$  is set larger than  $Z_F$  for harmonics, the combined method can eliminate the supply current harmonics  $I_{Sh}$  as effectively as the current-detecting method can. Note that the supply harmonic and/or flicker voltage  $V_{Sh}$  is excluded from (8). The first term on the right hand of (3) plays an essential role in harmonic current compensation of the load, while the second term contributes to voltage-flicker cancellation from

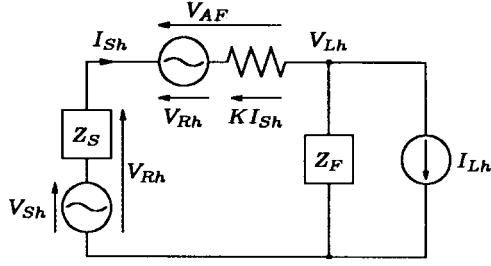


Fig. 6. Equivalent circuit for combined method.

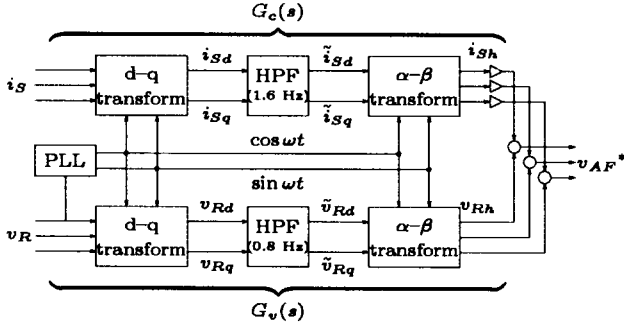


Fig. 7. Control circuit of series-active filter.

$V_{Lh}$ . Assuming that  $K$  is infinite, the output voltage of the series-active filter  $V_{AF}$  is given by

$$\lim_{K \rightarrow \infty} V_{AF} = Z_F I_{Lh} + V_{Sh}. \quad (10)$$

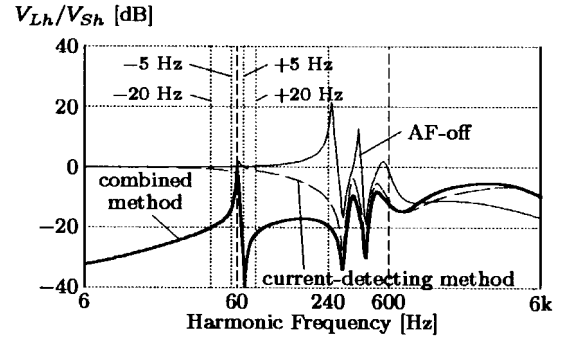
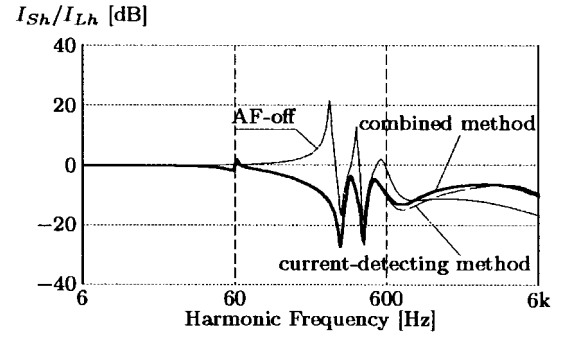
The feedback gain  $K$  in the combined method can be set lower than that in the current-detecting method because the voltage-detecting loop in the combined method compensates for the voltage flicker. For example, the passive filter used in the following experiments shows a capacitive impedance as high as  $4 \Omega$  for around the fundamental frequency, while it exhibits an impedance as low as  $0.07 \Omega$  for the 5th-harmonic frequency. Thus, the required gain in the current-detecting method would be 60 times as high as that in the combined method.

## V. COMPENSATING CHARACTERISTICS

### A. Control Circuit

Fig. 7 shows a control circuit of the series-active filter based on the combined control method of (3). The control circuit consists of two  $d$ - $q$  transformation circuits  $G_c(s)$  and  $G_v(s)$ , which take the detected three-phase supply current  $i_S$  and the detected three-phase receiving terminal voltage  $v_R$ , respectively.

Two first-order high-pass filters (HPF's) with cutoff frequencies of 1.6 Hz in  $G_c(s)$  are used for extraction of current harmonics  $i_{Sh}$ , while two more HPF's with cutoff frequencies of 0.8 Hz in  $G_v(s)$  are used for extraction of voltage flicker/imbalance  $v_{Rh}$ . The control gain  $K$  is set to 2  $\Omega$ . The control circuit is implemented in a DSP(TMS320C20).

Fig. 8. Compensation characteristics of  $V_{Lh}/V_{Sh}$ .Fig. 9. Compensation characteristics of  $I_{Sh}/I_{Lh}$ .

### B. Analysis of Compensating Characteristics

Fig. 8 shows a voltage harmonics/flicker ratio of the load terminal to the supply, which is given by

$$\left. \frac{V_{Lh}}{V_{Sh}} \right|_{I_{Lh}=0} = \frac{Z_F(1 - G_v)}{(1 - G_v)Z_S + Z_F + KG_c}. \quad (11)$$

When no series-active filter is connected (AF off), the supply harmonic voltage at 240 Hz is amplified by about ten times at the load terminal because of series resonance between  $Z_S$  and  $Z_F$ . After the series-active filter based on either the current-detecting method or the combined method is operated, no amplification occurs, that is, the ratio of  $V_{Lh}$  to  $V_{Sh}$  is less than 0 dB in either case.

However, these two methods are quite different in voltage-flicker compensating characteristics. The plots for the current-detecting method are nearly 0 dB in a frequency range of  $60 \pm 20$  Hz because the current-detecting method has almost no capability of voltage-flicker compensation in  $v_L$ . On the other hand, the plots for the combined method are  $-15$  to  $-20$  dB for voltage flicker with a frequency range of 5–20 Hz. This means that the combined method has the capability of voltage-flicker compensation of the supply.

Fig. 9 shows a ratio of supply current harmonics with respect to load current harmonics

$$\left. \frac{I_{Sh}}{I_{Lh}} \right|_{V_{Sh}=0} = \frac{Z_F}{(1 - G_v)Z_S + Z_F + KG_c}. \quad (12)$$

The plots for the current-detecting method are similar to those of the combined method. This means that the second term on the right hand of (3) makes no contribution to harmonic compensation.

## VI. FLOW OF INSTANTANEOUS ACTIVE AND REACTIVE POWERS

### A. Instantaneous Active and Reactive Powers in Series-Active Filter

Assuming that no shunt-active filter is installed, the flow of instantaneous active and reactive powers into or out of the series-active filter will be discussed, with emphasis on supply voltage flicker. Three-phase-balanced voltages  $\mathbf{v}_{Sf}$  are given by

$$\mathbf{v}_{Sf} = \begin{bmatrix} v_{Sfu} \\ v_{Sfv} \\ v_{Sfw} \end{bmatrix} = \sqrt{2}V_{Sf} \begin{bmatrix} \cos \omega t \\ \cos(\omega t - 2\pi/3) \\ \cos(\omega t + 2\pi/3) \end{bmatrix} \quad (13)$$

where

$V_{Sf}$  supply voltage amplitude;  
 $\omega$  supply angular frequency.

Because voltage flicker is considered a low-frequency amplitude modulation of the fundamental supply voltage, voltage flicker  $\Delta v_S$  in each phase is given as follows:

$$\Delta \mathbf{v}_S = \begin{bmatrix} \Delta v_{Su} \\ \Delta v_{Sv} \\ \Delta v_{Sw} \end{bmatrix} = \sqrt{2}\Delta v_S \begin{bmatrix} \cos \omega t \\ \cos(\omega t - 2\pi/3) \\ \cos(\omega t + 2\pi/3) \end{bmatrix} \quad (14)$$

where

$\Delta v_S = \Delta V_S \cos(\omega' t + \phi')$ ;  
 $\Delta V_S$  amplitude of supply voltage flicker;  
 $\omega'$  angular frequency of supply voltage flicker.

Hence, the supply voltage  $\mathbf{v}_S$  is given as a sum of  $\mathbf{v}_{Sf}$  and  $\Delta \mathbf{v}_S$

$$\mathbf{v}_S = \begin{bmatrix} v_{Su} \\ v_{Sv} \\ v_{Sw} \end{bmatrix} = \begin{bmatrix} v_{Sfu} \\ v_{Sfv} \\ v_{Sfw} \end{bmatrix} + \begin{bmatrix} \Delta v_{Su} \\ \Delta v_{Sv} \\ \Delta v_{Sw} \end{bmatrix}. \quad (15)$$

Because  $\Delta \mathbf{v}_S$  is canceled by the series-active filter, the load terminal voltage  $\mathbf{v}_L$  equals  $\mathbf{v}_{Sf}$ , so that no supply voltage flicker appears at the load terminal. Therefore, the load current  $\mathbf{i}_L$  has a constant amplitude of  $I_L$ , and the passive filter current  $\mathbf{i}_F$  has a constant amplitude of  $I_F$ .

With the series-active filter operating, the passive filter is assumed to sink all the load current harmonics. Here,  $p_L$  and  $q_L$  represent the instantaneous active and reactive powers of the load, and  $p_F$  and  $q_F$  are those of the passive filter. According to [9], instantaneous active power  $p_L$  ( $p_F = 0$ ) and instantaneous reactive power  $q_L + q_F$  on the side upstream of the load terminal are given by

$$\begin{bmatrix} p_L \\ q_L + q_F \end{bmatrix} = \begin{bmatrix} v_{Sf\alpha} & v_{Sf\beta} \\ -v_{Sf\beta} & v_{Sf\alpha} \end{bmatrix} \begin{bmatrix} i_{L\alpha} + i_{F\alpha} \\ i_{L\beta} + i_{F\beta} \end{bmatrix} = 3V_{Sf} \begin{bmatrix} I_L \cos \phi \\ I_L \sin \phi + I_F \end{bmatrix} \quad (16)$$

where

$\cos \phi$  displacement power factor of load.

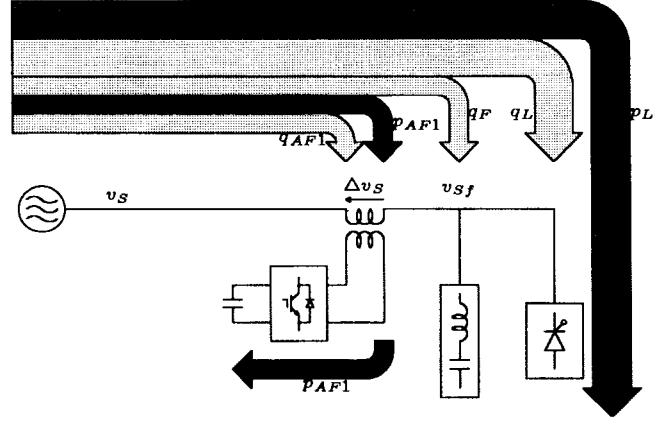


Fig. 10. Flow of instantaneous active and reactive powers when no shunt-active filter is installed.

Taking into account the output voltage of the series-active filter, instantaneous active power  $p_{AF1}$  and instantaneous reactive power  $q_{AF1}$  inside the series-active filter are obtained as follows:

$$\begin{bmatrix} p_{AF1} \\ q_{AF1} \end{bmatrix} = \begin{bmatrix} \Delta v_{S\alpha} & \Delta v_{S\beta} \\ -\Delta v_{S\beta} & \Delta v_{S\alpha} \end{bmatrix} \begin{bmatrix} i_{L\alpha} + i_{F\alpha} \\ i_{L\beta} + i_{F\beta} \end{bmatrix} = 3\Delta v_S \begin{bmatrix} I_L \cos \phi \\ I_L \sin \phi + I_F \end{bmatrix}. \quad (17)$$

The above equation means that  $p_{AF1}$  and  $q_{AF1}$  fluctuate at an angular frequency of  $\omega'$ .

On the supply side, instantaneous active power  $p_S$  and instantaneous reactive power  $q_S$  are given by

$$\begin{bmatrix} p_S \\ q_S \end{bmatrix} = \begin{bmatrix} v_{S\alpha} & v_{S\beta} \\ -v_{S\beta} & v_{S\alpha} \end{bmatrix} \begin{bmatrix} i_{S\alpha} \\ i_{S\beta} \end{bmatrix} = 3(V_{Sf} + \Delta v_S) \begin{bmatrix} I_L \cos \phi \\ I_L \sin \phi + I_F \end{bmatrix}. \quad (18)$$

Equation (18) equals the sum of (16) and (17) as

$$\begin{bmatrix} p_S \\ q_S \end{bmatrix} = \begin{bmatrix} p_{AF1} \\ q_{AF1} \end{bmatrix} + \begin{bmatrix} p_L \\ q_L + q_F \end{bmatrix}. \quad (19)$$

Fig. 10 shows the flow of instantaneous active and reactive powers when no shunt-active filter is connected. Note that  $p_L$ ,  $q_L$ , and  $q_F$  are constant values, while  $p_{AF1}$  and  $q_{AF1}$  fluctuate due to the supply voltage flicker of (14). The fluctuation of  $p_{AF1}$  results in the variation of the dc-link voltage at  $\omega'$  because no shunt-active filter is connected. The total amount of instantaneous active power drawn from the supply also fluctuates at  $\omega'$ . Note that  $q_{AF1}$  has no effect on the dc-link voltage [9].

Assuming that the dc-link voltage  $v_d$  is the sum of a fluctuating component  $\tilde{v}_d$  and a constant component  $V_d$ ,  $\tilde{v}_d$  is given by

$$\tilde{v}_d = \frac{1}{C} \int \frac{p_{AF1}}{v_d} dt = \frac{1}{C} \int \frac{3\Delta v_S I_L \cos \phi}{v_d} dt. \quad (20)$$

The following approximation exists as long as the fluctuation of  $\tilde{v}_d$  is much smaller than  $V_d$ :

$$\tilde{v}_d \doteq \frac{3\Delta V_S I_L \cos \phi}{\omega' C V_d} \sin(\omega' t + \phi'). \quad (21)$$

The ratio of  $\tilde{v}_d$  to  $V_d$ ,  $\varepsilon$  is given by

$$\varepsilon = \frac{3\Delta V_S I_L \cos \phi}{\omega' C V_d^2}. \quad (22)$$

Note that  $\varepsilon$  is inversely proportional to flicker frequency. This means that a larger capacity dc capacitor is required to compensate for voltage flicker fluctuating at a lower frequency.

### B. DC-Link Voltage Regulation

The purpose of the shunt-active filter is to inject instantaneous active power  $p_{AF2}$  into the supply and to keep instantaneous reactive power  $q_{AF2}$  at zero. Here,  $p_{AF2}$  is equal to  $p_{AF1}$ , so that no variation occurs in the dc-link voltage. Accordingly,  $p_{AF2}$  and  $q_{AF2}$  are given by

$$\begin{bmatrix} p_{AF2} \\ q_{AF2} \end{bmatrix} = \begin{bmatrix} p_{AF1} \\ 0 \end{bmatrix}. \quad (23)$$

Fig. 11 shows the flow of instantaneous active power when the shunt-active filter is operated. The instantaneous active power drawn from the supply  $p_S$  equals  $p_L$  because  $p_{AF2}$  and  $p_{AF1}$  cancel each other at the receiving terminal. Here,  $p_S$  and  $q_S$  are given by

$$\begin{aligned} \begin{bmatrix} p_S \\ q_S \end{bmatrix} &= \begin{bmatrix} p_L \\ q_L + q_F + q_{AF1} \end{bmatrix} \\ &= \begin{bmatrix} 3V_{Sf} I_L \cos \phi \\ 3(V_{Sf} + \Delta v_S)(I_L \sin \phi + I_F) \end{bmatrix}. \end{aligned} \quad (24)$$

Although voltage flicker  $\Delta v_S$  is superimposed on the supply voltage  $v_S$ ,  $p_S$  is constant, while  $q_S$  is not constant because  $q_{AF1}$  fluctuates. On the supply side, instantaneous active current  $i_{Sp}$  and instantaneous reactive current  $i_{Sq}$  can be derived from (26)

$$\mathbf{i}_{Sp} = \begin{bmatrix} i_{Spu} \\ i_{Spv} \\ i_{Spw} \end{bmatrix} = \frac{\sqrt{2}V_{Sf} I_L \cos \phi}{V_{Sf} + \Delta v_S} \begin{bmatrix} \cos \omega t \\ \cos(\omega t - \frac{2}{3}\pi) \\ \cos(\omega t + \frac{2}{3}\pi) \end{bmatrix} \quad (25)$$

$$\mathbf{i}_{Sq} = \begin{bmatrix} i_{Squ} \\ i_{Sqv} \\ i_{Sqw} \end{bmatrix} = \sqrt{2}(I_L \sin \phi + I_F) \begin{bmatrix} \sin \omega t \\ \sin(\omega t - \frac{2}{3}\pi) \\ \sin(\omega t + \frac{2}{3}\pi) \end{bmatrix}. \quad (26)$$

The amplitude of  $i_{Sp}$  varies although  $p_S$  is constant, whereas the amplitude of  $i_{Sq}$  is constant because  $\Delta v_S$  is excluded from (26).

## VII. EXPERIMENTAL RESULTS

Figs. 12–15 show experimental results obtained from Fig. 2 when the voltage flicker of 4%, which fluctuates at 5 Hz, is superimposed on the supply by the voltage-flicker/imbalance generator. Fig. 13 shows close-up waveforms of  $v_R$  and  $v_L$  in Fig. 12. With the help of the series-active filter, the amplitude

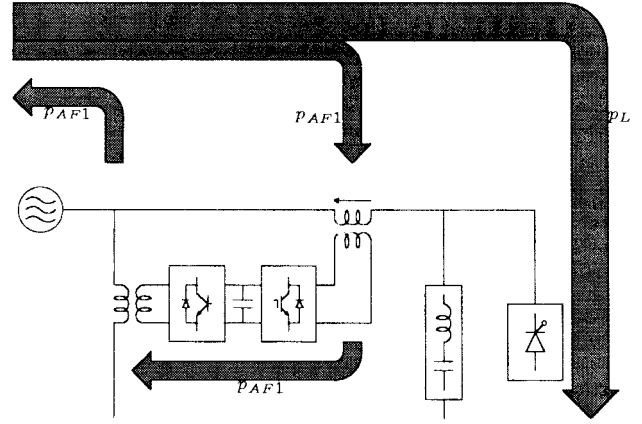


Fig. 11. Flow of instantaneous active power when shunt-active filter is operated.

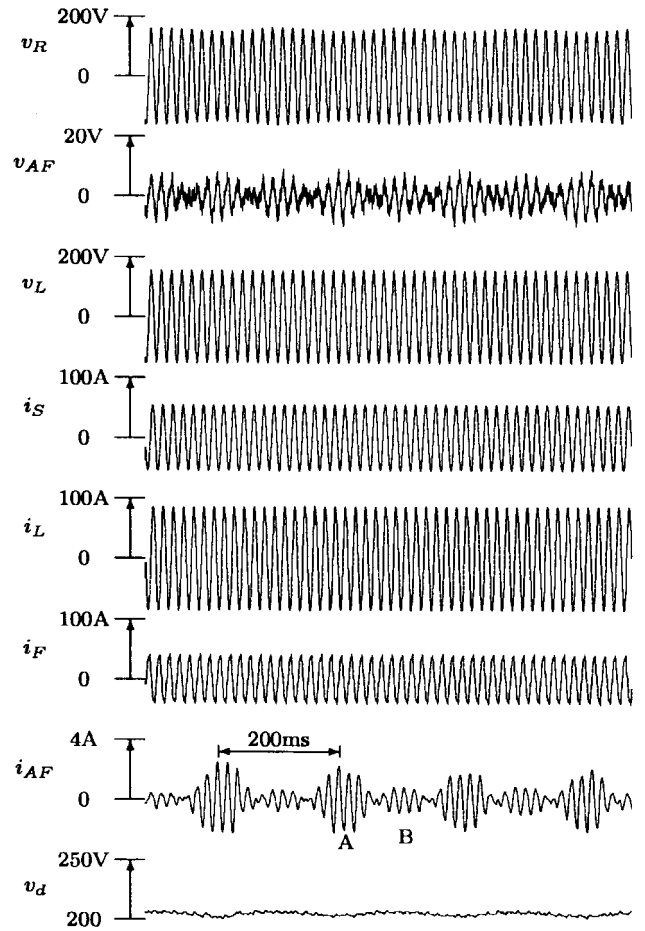


Fig. 12. Experimental waveforms.

variation in  $v_L$  is reduced to 1/10, compared to that in  $v_R$ . The rms voltage of the series-active filter is 4.4 V (3.8%) of the supply, which is equal to the rms voltage of the supply flicker. The rms current of  $i_L$  is 60 A, and the displacement power factor of the load is  $\cos \phi = 0.45$ , hence, the fluctuating active power flowing into the series-active filter is given by

$$3 \times 4.4^2 \times 60^2 \times 0.45 = 360 \text{ W}.$$

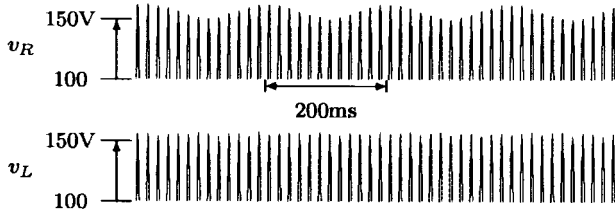
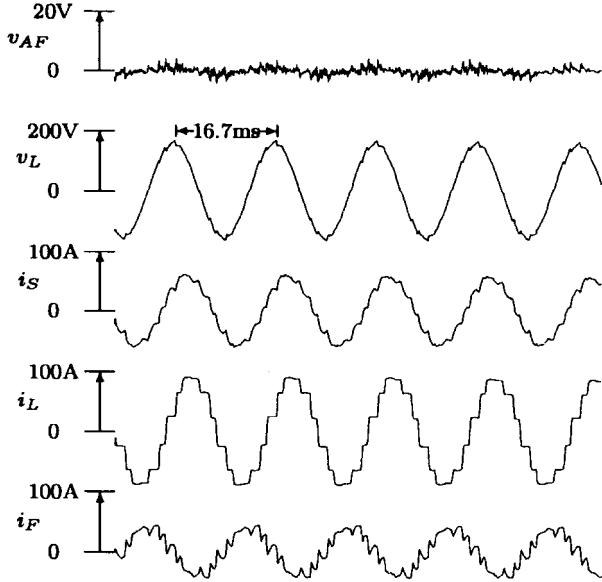
Fig. 13. Close-up waveform of  $v_R$  and  $v_L$ .

Fig. 14. Experimental waveforms before both active filters are operated.

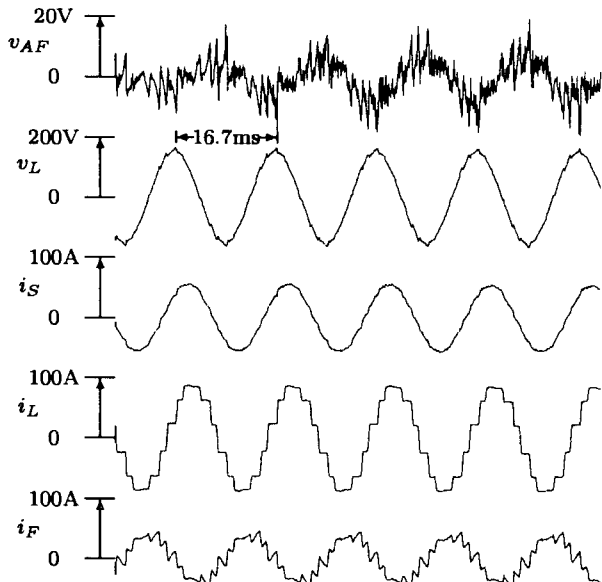


Fig. 15. Experimental waveforms after both active filters are operated.

The shunt-active filter injects  $i_{AF}$  into the supply, the amplitude of which fluctuates due to the voltage flicker in  $v_S$ . The variation of the dc-link voltage is suppressed within only 2 V (1%). This means that the shunt-active filter returns almost all the active power drawn by the series-active filter to the supply. If the shunt-active filter is disconnected, the

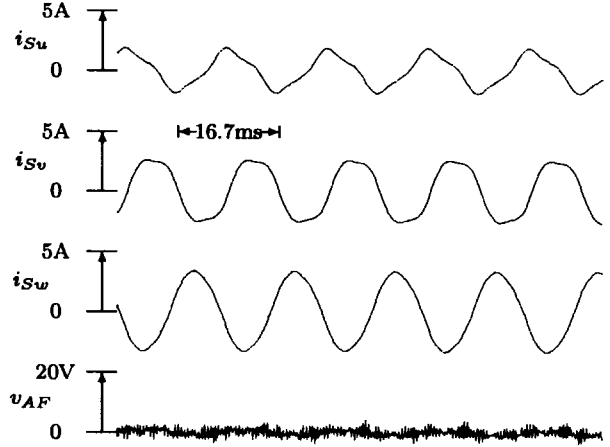


Fig. 16. Experimental waveforms under voltage imbalance condition before starting series-active filter.

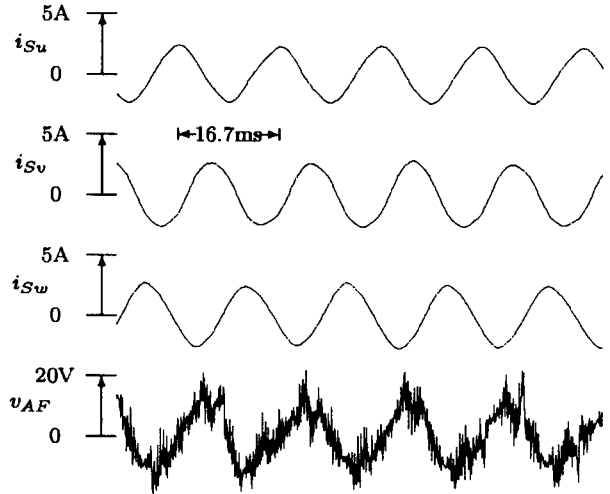


Fig. 17. Experimental waveforms under voltage imbalance condition after starting series-active filter.

variation of the dc-link voltage reaches

$$\begin{aligned} \varepsilon &= \frac{3\Delta V_S I_L \cos \phi}{\omega' C V_d^2} \\ &= \frac{20 \times 10^3 \times 3.8/100 \times 1}{2\pi \times 5 \times 2000 \times 10^{-6} \times 200^2} = 13\%. \end{aligned}$$

The active power of 520 W flows into the shunt-active filter at Point A in Fig. 12, while the active power of 170 W flows out at Point B. Thus, the variation of active power is  $(520 - 170)/2 = 345$  W. This is equal to nearly 360 W.

Figs. 14 and 15 are experimental waveforms before and after starting the series-active filter. The supply current  $i_S$  in Fig. 14 includes a nonnegligible amount of 11th and 13th harmonic currents. On the other hand,  $i_S$  in Fig. 15 is a purely sinusoidal waveform.

Figs. 16 and 17 show experimental waveforms under an imbalance condition with a negative-sequence voltage of 4% superimposed on the supply voltage by the voltage-flicker/imbalance generator. Here, an induction motor of 2.2 kW is connected as a load, which presents a low impedance at the negative sequence. Before starting the series-active filter,



the three-phase load currents include a negative-sequence current of 1 A. After starting, the negative-sequence current becomes 0.2 A because the negative sequence in the load terminal voltage is reduced from 4% to less than 1%.

### VIII. CONCLUSION

This paper has dealt with UPQC's, the aim of which is not only to compensate for current harmonics produced by nonlinear loads, but also to eliminate voltage flicker/imbalance appearing at the receiving terminal from the load terminal. Theoretical comparison among three types of control methods for the series-active filter has clarified that the combination of current and voltage-detecting methods is suitable for voltage-flicker/imbalance elimination and harmonic compensation. The flow of instantaneous active and reactive powers has shown that installation of the shunt-active filter is effective in performing dc-voltage regulation.

Although the specific UPQC dealt with in this paper provides no power factor correction in order to minimize the required rating of the shunt-active filter, the general UPQC is capable of improving "power quality" as well as improving power factor.

### REFERENCES

- [1] H. Akagi, "New trends in active filters for power conditioning," *IEEE Trans. Ind. Applicat.*, vol. 32, no. 6, pp. 1312–1322, 1996.
- [2] S. Moran, "A line voltage regulator/conditioner for harmonic sensitive load isolation," in *1989 IEEE/IAS Annu. Meet.*, pp. 947–951.
- [3] F. Kamran and T. G. Habetler, "Combined deadbeat control of a series-parallel converter combination used as a universal power filter," in *1995 IEEE Power Electronics Specialist Conf.*, pp. 196–201.
- [4] F. Z. Peng, H. Akagi, and A. Nabae, "A new approach to harmonic compensation in power systems—A combined system of shunt passive and series active filters," *IEEE Trans. Ind. Applicat.*, vol. 26, no. 6, pp. 983–990, 1990.
- [5] H. Fujita and H. Akagi, "A practical approach to harmonic compensation in power systems—Series connection of passive and active filters," *IEEE Trans. Ind. Applicat.*, vol. 27, no. 6, pp. 1020–1025, 1991.
- [6] S. Bhattacharya and D. M. Divan, "Synchronous frame based controller implementation for a hybrid series active filter system," *IEEE/IAS Annu. Meet.*, 1995, pp. 2531–2540.
- [7] E. H. Watanabe, "Series active filter for the DC Side of HVDC transmission systems," in *Proc. 1990 Int. Power Electronics Conf.*, Tokyo, Japan, 1990, pp. 1024–1030.
- [8] L. Gyugyi, "A unified flow control concept for flexible AC transmission systems," *Proc. Inst. Elect. Eng.*, vol. 139, pt. C, no. 4, pp. 323–331, 1992.
- [9] H. Akagi, Y. Kanazawa, and A. Nabae, "Instantaneous reactive power compensators comprising switching devices without energy storage components," *IEEE Trans. Ind. Applicat.*, vol. 20, no. 3, pp. 625–630, 1984.



**Hideaki Fujita** (M'91) was born in Toyama Prefecture, Japan, on September 10, 1965. He received the B.S. and M.S. degrees in electrical engineering from the Nagaoka University of Technology, Japan, in 1988 and 1990, respectively.

Since 1991, he has been a Research Associate in the Department of Electrical Engineering, Okayama University, Okayama, Japan. His research interests are static var compensators, active power filters, and resonant converters.

Mr. Fujita received two First Prize Paper Awards from the Industrial Power Converter Committee in the IEEE Industry Applications Society in 1990 and 1995.



**Hirofumi Akagi** (M'87–SM'94–F'96) was born in Okayama-City, Japan, on August 19, 1951. He received the B.S. degree from the Nagoya Institute of Technology, Nagoya, Japan, in 1974 and the M.S. and Ph.D. degrees from the Tokyo Institute of Technology, Tokyo, Japan, in 1976 and 1979, respectively, all in electrical engineering.

In 1979, he joined the Nagaoka University of Technology as an Assistant and then Associate Professor in the Department of Electrical Engineering. In 1987, he was a Visiting Scientist at the Massachusetts Institute of Technology, Cambridge, MA, for ten months. Since 1991, he has been a Full Professor in the Department of Electrical Engineering, Okayama University, Okayama, Japan. From March to August of 1996, he was a Visiting Professor at the University of Wisconsin, Madison, and then the Massachusetts Institute of Technology. His research interests include ac motor drives, high-frequency resonant inverters for induction heating and corona discharge treatment, and utility applications of power electronics such as active filters, static var compensators, and FACTS devices.

Dr. Akagi has received seven IEEE/IAS society and committee prize paper awards, including the First Prize Paper Award in the IEEE TRANSACTIONS ON INDUSTRY APPLICATIONS for 1991. He is a Distinguished Lecturer of the IEEE/IAS for 1998–1999.